AD-A115 596 COLD REGIONS RESEARCH AND ENGINEERING LAB HANOVER NH F/G 4/2
SENSIBLE AND LATENT HEAT FLUXES AND HUMIDITY PROFILES FOLLOWING--ETC(U)
APR 82 E L ANDREAS
UNCLASSIFIED CRREL-82-12 NL

END
DATE FILMED
07-82
DTIC

CRREL

REPORT 82-12

US Army Corps of Engineers
Cold Regions Research & Engineering Laboratory

- AD A115596

Sensible and latent heat fluxes and humidity profiles following a step change in surface moisture

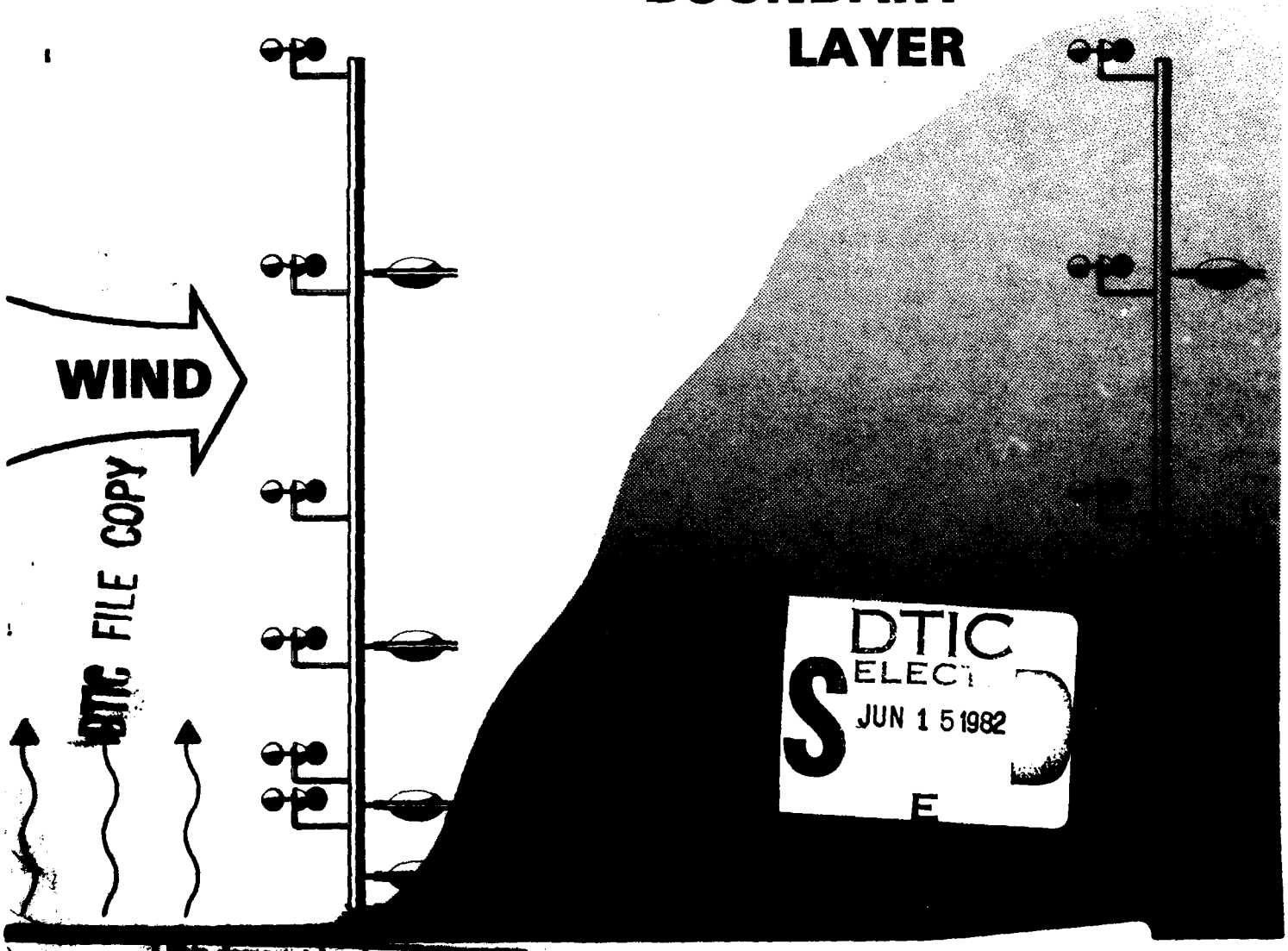

For conversion of SI metric units to U.S./ British customary units of measurement consult ASTM Standard E380, Metric Practice Guide, *published by the American Society for Testing and Materials, 1916 Race St., Philadelphia, Pa. 19103.*

CRREL Report 82-12

April 1982

Sensible and latent heat fluxes and humidity profiles following a step change in surface moisture

Edgar L. Andreas

Accession For	
NTIS GRA&I	X
DTIC TAB	☐
Unannounced	☐
Justification	
By	
Distribution/	
Availability Codes	
Dist	Avail and/or Special
A	

Prepared for
OFFICE OF THE CHIEF OF ENGINEERS

Unclassified
SECURITY CLASSIFICATION OF THIS PAGE (When Data Entered)

REPORT DOCUMENTATION PAGE

READ INSTRUCTIONS BEFORE COMPLETING FORM

1. REPORT NUMBER: CRREL Report 82-12
2. GOVT ACCESSION NO.: AD-A115 596
3. RECIPIENT'S CATALOG NUMBER:
4. TITLE (and Subtitle): SENSIBLE AND LATENT HEAT FLUXES AND HUMIDITY PROFILES FOLLOWING A STEP CHANGE IN SURFACE MOISTURE
5. TYPE OF REPORT & PERIOD COVERED:
6. PERFORMING ORG. REPORT NUMBER:
7. AUTHOR(s): Edgar L Andreas
8. CONTRACT OR GRANT NUMBER(s):
9. PERFORMING ORGANIZATION NAME AND ADDRESS: U.S. Army Cold Regions Research and Engineering Laboratory, Hanover, New Hampshire 03755
10. PROGRAM ELEMENT, PROJECT, TASK AREA & WORK UNIT NUMBERS: DA Project 4A161102AT24, Technical Area C, Scientific Area 01, Work Unit 004
11. CONTROLLING OFFICE NAME AND ADDRESS: Office of the Chief of Engineers, Washington, D.C. 20314
12. REPORT DATE: April 1982
13. NUMBER OF PAGES: 24
14. MONITORING AGENCY NAME & ADDRESS (if different from Controlling Office):
15. SECURITY CLASS. (of this report): Unclassified
15a. DECLASSIFICATION/DOWNGRADING SCHEDULE:
16. DISTRIBUTION STATEMENT (of this Report): Approved for public release; distribution unlimited.
17. DISTRIBUTION STATEMENT (of the abstract entered in Block 20, if different from Report):
18. SUPPLEMENTARY NOTES:
19. KEY WORDS (Continue on reverse side if necessary and identify by block number):
Heat flux
Humidity
Micrometeorology
Surface properties
20. ABSTRACT (Continue on reverse side if necessary and identify by block number):

From a high-quality set of velocity, temperature, and humidity profiles collected upwind and downwind of a step change in surface roughness, temperature, and moisture, we have calculated upwind and downwind values of the heat fluxes and friction velocity. The surface change is from smooth to rough; upwind, the sensible heat flux is upward and the latent heat flux is zero; downwind, the surface is well-watered so that the latent heat flux is upward while the sensible heat flux is downward. The downwind latent heat flux in this fetch-limited flow obeys $N_L = 0.08\ R_x^{0.76}$ where N_L is the latent heat Nusselt number and R_x is the fetch Reynolds number, a parameter for characterizing fetch-limited flows. Because this relation is virtually the same as one found to describe the sensible heat and condensate fluxes over arctic leads, we conclude that the Nusselt numbers nondimensionalizing scalar fluxes are the same for a given fetch

DD FORM 1 JAN 73 1473 EDITION OF 1 NOV 65 IS OBSOLETE

Unclassified
SECURITY CLASSIFICATION OF THIS PAGE (When Data Entered)

20. Abstract (cont't)

Reynolds number when boundary conditions are similar. This Nusselt number equality implies that Nusselt numbers are more fundamental flux parameters than the bulk aerodynamic coefficients in fetch-limited flows. The humidity-difference profiles (downwind minus upwind) obey $[-\Delta Q(z)/q_*]^{1/2} = -0.37 \ln(z/h)$ where q_* is a humidity scale—the friction humidity— and h is an estimator of internal boundary layer height. This humidity-difference profile is essentially the same as that found to fit condensate profiles at the downwind edge of arctic leads. Humidity and condensate in these two flows are unaffected by buoyancy and for each the corresponding upwind flux is constant (zero) with height.

PREFACE

This report was prepared by Dr. Edgar L. Andreas, Physicist, of the Physical Sciences Branch, Research Division, U.S. Army Cold Regions Research and Engineering Laboratory. Funding for this research was provided by DA Project 4A161102AT24, *Research in Snow, Ice and Frozen Ground*, Technical Area C, *Research in Terrain and Climatic Constraints*, Scientific Area 01, *Cold Environment Factors*, Work Unit 004, *Cold Regions Surface Boundary Layer Physics and Chemistry*.

The author thanks R. Bates and W. Tucker of CRREL for technically reviewing the manuscript of this report, and Dr. J. Schreffler of the Environmental Protection Agency for providing a complete copy of the data table (Table 1) of Rider, Philip, and Bradley (1963).

CONTENTS

ILLUSTRATIONS

TABLES

LIST OF SYMBOLS

C	condensate concentration profile (in g/g)
c	turbulent condensate fluctuation
C_{02}	downwind surface condensate concentration
C_{200}	condensate concentration 200 cm above the upwind surface
c_e	specific heat of tarmac
c_p	specific heat of air
c_*	condensate concentration scale (in g/g) defined from the surface value of the condensate flux
$\hat{c}$	condensate concentration scale dependent on the two length scales z and h
D	thermal diffusivity of air
D_S	molecular diffusivity of an arbitrary scalar S
D_w	molecular diffusivity of water vapor in air
d	thickness of tarmac that undergoes surface heating
$\bar{e}$	$= \overline{u^2} + \overline{v^2} + \overline{w^2}$, the turbulent kinetic energy
G	conductive flux into the ground
g	acceleration of gravity
H_c	downwind surface condensate flux
H_L	latent heat flux at the surface
H_{L2}	latent heat flux at the downwind surface
H_S	kinematic surface flux of an arbitrary scalar S
H_s	sensible heat flux at the surface
H_{sj}	sensible heat flux at the upwind ($j = 1$) or downwind ($j = 2$) surface
h	estimator of internal boundary layer height
K	$= \frac{1}{2}(\overline{w^2}\bar{e}/\epsilon\Lambda)$, a model of the turbulent diffusivity
k	von Kármán's constant
L	Obukhov length corrected for the moisture flux
L_v	latent heat of vaporization of water
N	Nusselt number
N_c	Nusselt number for the condensate flux
N_L	Nusselt number for the latent heat flux
N_S	Nusselt number for the flux of an arbitrary scalar S
N_s	Nusselt number for the sensible heat flux
P	$= \nu/D$, the Prandtl number
Q	downwind profile of specific humidity (in g/kg)
q	turbulent humidity fluctuation
Q_i	upwind humidity profile
Q_{02}	downwind surface humidity

Q_{200}	specific humidity 200 cm above the upwind surface
q_*	$= -H_{L2}/\rho L_v k\, u_{*down}$, a specific humidity scale (in g/kg)
R_L	incident longwave radiation
R_n	net radiation
R_{nj}	net radiation upwind ($j = 1$) or downwind ($j = 2$)
R_s	incident shortwave radiation
R_x	$= U_{200}X/\nu$, the fetch Reynolds number
R_*	$= u_* z_0/\nu$, the roughness Reynolds number
S	profile of an arbitrary scalar quantity
S_0	surface value of the scalar S
S_{200}	value of the scalar S 200 cm above the upwind surface
Sc	$= \nu/D_w$, the Schmidt number
St_L	Stanton number for the latent heat flux
St_s	Stanton number for the sensible heat flux
$\tilde{S}$	$= (S - S_{200})/(S_0 - S_{200})$, the nondimensional value of the arbitrary scalar S
T	downwind profile of temperature
T_i	upwind temperature profile
T_0	temperature representative of the surface layer
T_{0j}	surface temperature
T_{27}	temperature 27.5 cm above the upwind surface
T_{200}	temperature 200 cm above the upwind surface
U	downwind profile of wind speed
u	turbulent longitudinal velocity fluctuation
U_i	upwind profile of wind speed
U_{50}	wind speed 50 cm above the surface at fetch X
U_{200}	wind speed 200 cm above the upwind surface
u_*	$= (\tau/\rho)^{1/2}$, the friction velocity
u_{*up}	upwind friction velocity
u_{*down}	downwind friction velocity
v	turbulent transverse velocity fluctuation
W	mean vertical velocity
w	turbulent vertical velocity fluctuation
$\overline{wc}$	turbulent condensate flux
$\overline{wq}$	turbulent humidity flux
$\overline{wq}_i$	turbulent upwind humidity flux
$\overline{w\theta}$	turbulent temperature flux
$\overline{w\theta}_i$	turbulent upwind temperature flux
X	fetch measured downwind from the surface change
x	longitudinal space coordinate, with $x = 0$ being where the surface changes
$\tilde{x}$	$= x/X$, the nondimensional longitudinal coordinate
y	$= [1 - 16(z/L)]^{1/4}$
z	vertical space coordinate
z_h	roughness length for temperature
z_w	scalar roughness length for humidity or condensate

z_0	roughness length for wind speed
z_{02}	downwind roughness length
z'	arbitrary height greater than the height of the internal boundary layer at fetch X
$\tilde{z}$	$= (z^2 U_{200}/\nu x)^{1/2}$, the nondimensional height
α_j	surface albedo
ΔQ	$= Q(X,z) - Q_i(z)$, the profile of downwind minus upwind humidity
δ	internal boundary layer height
δ_h	height of the thermal internal boundary layer
δ_q	height of the moisture internal boundary layer
ϵ	dissipation rate of turbulent kinetic energy
ϵ_j	surface emissivity
θ	turbulent temperature fluctuation
θ_*	$= -\overline{w\theta}_j/k\, u_*$, an upwind temperature scale
κ	thermal conductivity of air
Λ	dimensionless constant
ν	kinematic viscosity of air
ρ	density of air
ρ_e	density of tarmac
$\rho_{\theta q}$	$= \overline{\theta q}/\sigma_\theta\, \sigma_q$, the temperature-humidity correlation coefficient
σ	Stefan-Boltzmann constant
σ_q	standard deviation of humidity
σ_w	standard deviation of vertical velocity
σ_θ	standard deviation of temperature
τ	surface stress
ϕ_c	nondimensional condensate gradient
ψ_h	stability correction to the temperature profile
ψ_m	stability correction to the wind speed profile

Subscript j can be either 1 or 2, where 1 denotes values appropriate over the upwind surface and 2, values over the downwind surface.

An overbar indicates a time average.

SENSIBLE AND LATENT HEAT FLUXES AND HUMIDITY PROFILES FOLLOWING A STEP CHANGE IN SURFACE MOISTURE

Edgar L. Andreas

INTRODUCTION

The velocity, temperature, and humidity profiles of Rider, Philip, and Bradley (1963), hereafter referred to as RPB, are an ideal set for testing models of air flow encountering an abrupt change in surface conditions and have been used several times for this purpose (Townsend 1965, Taylor 1971, Rao et al. 1974). Briefly, RPB studied the modification in a flow blowing from a hot, smooth tarmac airport runway onto a well-watered, grassy field (Fig. 1) at Canberra, Australia. Their data set includes temperature and humidity at five heights, between 5 and 150 cm, upwind and at several fetches downwind of the surface change, a velocity profile that is the average of the upwind profile and the downwind profile 16 m from the surface change, and measurements of upwind and downwind net all-wave radiation, ground heat flux, and radiative surface temperature.

Their data set is so complete that RPB could report on only a fraction of the possible computations it allows. Sibbons (Rider et al. 1965) pointed out a few of their omissions. The most obvious are calculations of the upwind and downwind sensible and latent heat fluxes. RPB did discuss the average downwind latent heat flux but did not report fluxes for individual runs. Thus, when Rao et al. (1974) used the data set in their numerical model, they based surface flux estimates on the net radiation and ground flux values that RPB did report. In testing his model, however, Taylor (1971) calculated the upwind sensible heat flux for two runs from the given profiles and found these values smaller than the sum of the net radiation and ground heat flux. Another look at the RPB data set, with emphasis on computing the surface heat fluxes from the reported profiles, would therefore be valuable.

I also have two personal reasons for looking at the data. Andreas et al. (1979) measured the sensible heat flux over arctic leads in winter and found that this flux obeyed

$$N_s = 0.14\, R_x^{0.72}, \qquad (1)$$

where N_s is the sensible heat flux Nusselt number and R_x is the fetch Reynolds number. Their attempt to measure latent heat flux was unsuccessful, however; they simply had to assume that temperature and moisture were transferred similarly—that the latent heat flux Nusselt number also obeys eq 1. In the flow RPB studied there was a large step increase in latent heat flux downwind of a uniform surface with negligible flux—just what occurs over leads. I therefore hope that the RPB data will help us better understand heat transfer from leads.

The high quality RPB humidity profiles also interest me. Andreas et al. (1981) reported that over arctic leads the condensate concentration profile, $C(z)$, obeys the relation

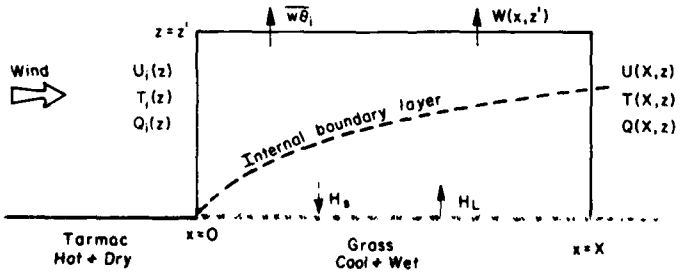

Figure 1. Internal boundary layer over the downwind grass.

$$[-C(z)/c_*]^{1/2} = -0.34 \ln(z/h), \quad (2)$$

where c_* is a concentration scale formed from the condensate flux, and h is an estimator of internal boundary layer height that depends on fetch. Since this was the first report of such a profile form, we seek confirmation. Andreas et al. (1981) inferred that the form of eq 2 was distinctly different from that of the temperature profiles over leads because condensate was transferred passively while tempera- was not. Because humidity was similarly passive in the regime RPB studied, I look for evidence in their downwind humidity profiles to support eq 2.

MATHEMATICAL

Upwind: flux-gradient method

The surface energy budget for steady-state conditions is

$$R_n - G = H_s + H_L . \quad (3)$$

Here I have followed Munn's (1966) sign convention: a gain in surface energy from net radiation, R_n, is positive; a ground flux, G, into the ground is positive; the turbulent sensible (H_s) and latent (H_L) heat fluxes are both positive when upward. RPB reported R_n both over the tarmac and 16 m downwind over the wet grass. They measured G at these same locations for 25 of their 43 experimental runs. I will calculate H_s and H_L from their velocity, temperature, and humidity profiles.

The calculations are complicated because RPB reported a velocity profile that is the average of upwind and downwind profiles. From their Figure 5 and Figure 1 in Rider et al. (1965), the downwind velocities, especially in the lowest meter, clearly were lower than upwind velocities. Using their average profile would, therefore, bias both upwind and downwind flux calculations: I need individual upwind and downwind profiles. Because the two figures mentioned show that upwind and downwind profiles were virtually identical for heights above 1 m, the individual profiles can be retrieved from the average velocity profiles RPB tabulated by the flux-gradient method (Businger et al. 1971). I simply assume that over the uniform tarmac both upwind velocity and temperature profiles obeyed Monin-Obukhov similarity and fit them with empirical similarity functions.

There admittedly is still no universal agreement over the forms of these similarity functions (Yaglom 1977), but Wieringa's (1980) recent analysis of the effects of flow distortion on the Kansas results (Businger et al. 1971)—the most discordant of the published similarity functions—has resolved the main points of controversy. For the unstable flow upwind, I use the integrated similarity functions from Paulson (1970):

$$U(z) = u_* k^{-1} [\ln(z/z_0) - \psi_m(z/L)] \quad (4)$$

and

$$T(z) = T_{01} + \theta_* [\ln(z/z_h) - \psi_h(z/L)], \quad (5)$$

where

$$\psi_m = 2 \ln[(1+y)/2] + \ln[(1+y^2)/2] - 2 \arctan y + \pi/2, \quad (6)$$

$$\psi_h = 2 \ln[(1+y^2)/2], \quad (7)$$

$$y = [1 - 16(z/L)]^{1/4} . \quad (8)$$

The Obukhov length corrected for moisture flux (Zilitinkevich 1966, Busch 1973), a measure of surface-layer stability, is

$$L = -\frac{T_{27}}{g} \frac{u_*^3}{k \overline{w\theta_i}} \times \left[1 + \frac{0.61\, T_{27}}{1 + 0.61\, Q_i} \frac{\overline{wq_i}}{\overline{w\theta_i}}\right]^{-1} . \quad (9)$$

I fitted eqs 4 and 5 with the RPB upwind temperature data at z = 5, 11.5, 27.5, 64, 150 cm and with the velocity data at z = 100, 150, 200 cm—levels that I believe reflect the upwind velocity—and at z_0, where $U(z_0) = 0$.

The flux-gradient method is an iterative procedure. I initially assume neutral stability—that is, $z/L = 0$, then $\psi_m = \psi_h = 0$—and make a least-squares fit of the data compatible with the models, eqs 4 and 5. The slopes of the least-squares lines yield estimates of u_* and θ_* from which I can estimate z/L and, in turn, ψ_m and ψ_h. Using these ψ_m and ψ_h values in eqs 4 and 5, I again pass least-squares lines through the data. More accurate values of u_* and θ_* result. The process continues until the relative sum of squared profile deviations changes by less than 0.5% between consecutive iterations. This usually occurs after no more than five iterations.

RPB gave 0.002 cm as the upwind value of z_0. Taylor (1971) questioned the smallness of this number, however; with z_0 = 0.002 cm, the roughness Reynolds

number, $R_* = u_* z_0/\nu$, is 0.2 ~ 0.3, barely above the upper limit for *aerodynamically smooth flow*, 0.13, and well below the lower limit for *aerodynamically rough flow*, 2.5 (Businger 1973). In using $z_0 = 0.002$ cm I find that the flux-gradient iteration does not accurately reproduce the upwind and downwind profiles shown in Figure 5 of RPB or Figure 1 of Rider et al. (1965). The value $z_0 = 0.01$ cm, a roughness length consistent with ones reported for similar surfaces, yields upwind and downwind velocity profiles that agree well with the available profiles (i.e., Figure 5 of RPB and Figure 1 in Rider et al. 1965).

In eq 5 T_{01} is assumed to be the surface temperature of the tarmac. After calculating θ_* we can estimate T_{01} by assigning a value to z_h, the roughness length for temperature. I find that with $z_h = 0.2$ cm, T_{01} values computed with eq 5 are usually within 2°C of the radiative temperatures measured by RPB and also agree well with Sibbon's (Rider et al. 1965) calculations of T_{01} for runs 6 and 7.

These estimates of T_{01} permit evaluation of the downwind surface temperatures T_{02} from the net radiation values tabulated by RPB. I simply decompose the upwind and downwind values of net radiation into shortwave and longwave components (Munn 1966):

$$R_{n1} = (1 - \alpha_1)R_s + R_L - \epsilon_1 \sigma T_{01}^4 , \qquad (10)$$

$$R_{n2} = (1 - \alpha_2)R_s + R_L - \epsilon_2 \sigma T_{02}^4 . \qquad (11)$$

In these R_s is the incident shortwave radiation; α_j, the surface albedo ($j = 1,2$); R_L, the incident longwave radiation; and $\epsilon_j \sigma T_{0j}^4$, the emitted longwave radiation. RPB stated that within the accuracy of their measurements $\alpha_1 = \alpha_2$. Hence, eqs 10 and 11 show that

$$T_{02} = \left[(R_{n1} - R_{n2})/\sigma\epsilon_2 + (\epsilon_1/\epsilon_2)T_{01}^4\right]^{1/4} . \qquad (12)$$

With realistic values for the emissivity, $\epsilon_1 = 0.95$ and $\epsilon_2 = 0.99$ (Kondratyev 1969, Siegel and Howell 1971, Razumovskii and Popov 1974), eq 12 yields values of T_{02} 8°C lower, on the average, than the radiative temperatures RPB listed. My T_{02} values for Runs 6 and 7 do, however, agree very well with Sibbon's estimates (Rider et al. 1965). The downwind temperature and humidity profiles imply that my values of T_{02} are more reasonable than those RPB tabulated. Their downwind radiative temperatures are usually higher than the temperature at the lowest downwind profile level. This not only necessitates a complex shape for the temperature profile near the surface but also implies a positive sensible heat flux over the grass, a result incompatible with the shape of the downwind temperature profile. When compared with several RPB profile sets, the numerical models of Taylor (1971) and Rao et al. also predicted downwind surface temperatures consistently lower than those RPB listed in their Table 2.

The downwind humidity profiles confirm the accuracy of my downwind surface temperature values. In the heat flux calculations that follow I use for the downwind surface humidity Q_{02} the value resulting from an extrapolation according to eq 37 through the lowest two profile levels to $z_{02} = 0.14$ cm. Andreas et al. (1981) used this same extrapolation to calculate surface condensate concentrations over leads. The resulting values are always near the humidities computed assuming saturation with a surface at temperature T_{02}. If, on the other hand, the RPB surface temperatures were used, the surface relative humidity would generally be about 70%, contrary to the assumption by RPB and Sibbons (Rider et al. 1965) that the air is saturated over the wet grass.

Downwind: integral method

An internal boundary layer (IBL) developed when air that was essentially in equilibrium with the hot, dry tarmac runway encountered the cool, moist grass (Fig. 1). Air within the IBL was modified by the fluxes from the new surface, while the air above was unmodified. The existence of an IBL is the basis for my calculation of the downwind fluxes.

Consider a control volume over the downwind grass as shown in Figure 1. The top of this volume is at $z = z'$, where z' is greater than the IBL height $\delta(x)$ for all x. Andreas et al. (1979, 1981) have used the fact that the heat and mass content of this volume is constant in steady-state conditions to derive relations between surface fluxes and profiles measured at the upwind and downwind ends of the control volume. For completeness, I will go through an abbreviated derivation here; to fill in gaps, the reader can refer to Andreas et al. (1979, 1981).

The heat budget of the control volume is

$$\rho\int_0^{z'} U_i(z)[c_p T_i(z) + L_v Q_i(z)]\, dz + \int_0^{X} [H_s(x) + H_L(x)]\, dx - \rho\int_0^{X} W(x,z')[c_p T_i(z') + L_v Q_i(z')]\, dx$$

$$- \rho \int_0^X (c_p \overline{w\theta}_i + L_v \overline{wq}_i)\, dx$$

$$- \rho \int_0^{z'} U(X,z)[c_p T(X,z)$$

$$+ L_v Q(X,z)]\, dz = 0 . \qquad (13)$$

Here U, W, T, and Q are average values of longitudinal and vertical velocity, temperature, and specific humidity; w, θ, and q are the turbulent fluctuations of these; ρ and c_p are the density and specific heat of air; L_v is the latent heat of vaporization of water; and X is the fetch at which the downwind measurements were made. Subscript i denotes upwind (initial) conditions, so $\overline{w\theta}_i$ and $\overline{wq}_i$ are the turbulent upwind fluxes. $H_s(x)$ and $H_L(x)$ are the downwind surface fluxes of sensible and latent heat.

Although the RPB upwind humidity profiles consistently show a slight increase in humidity with height at the lowest levels, Rider et al. (1965) explained that this may have been a consequence of a systematic instrument error and so reiterated their earlier conclusion that $\overline{wq}_i$ was zero. Then, also, $Q_i(z) = Q_i(z') = Q_i$. Finally, using the integrated, two-dimensional continuity equation, we can eliminate $W(x,z')$ from eq 13, which thus reduces to

$$\int_0^X \{[H_s(x) - \rho c_p \overline{w\theta}_i] + H_L(x)\}\, dx$$

$$= \rho \int_0^{z'} U(X,z)\{c_p[T(X,z) - T_i(z)]$$

$$+ L_v[Q(X,z) - Q_i]\}\, dz$$

$$+ \rho c_p \int_0^{z'} [U(X,z) - U_i(z)][T_i(z)$$

$$- T_i(z')]\, dz . \qquad (14)$$

On estimating integrands in eq 14, it is evident that the entire second integral on the right-hand side is negligible in comparison to the first integral and I henceforth will ignore it.

Repeating the same analysis for the mass (water) budget of the control volume yields

$$L_v^{-1} \int_0^X H_L(x)\, dx$$

$$= \rho \int_0^{z'} U(X,z)[Q(X,z) - Q_i]\, dz . \qquad (15)$$

Consequently, the sensible and latent heat budgets of the volume are separable:

$$\int_0^X H_s(x)\, dx = \rho c_p \overline{w\theta}_i X$$

$$+ \rho c_p \int_0^{\delta_h(X)} U(X,z)[T(X,z) - T_i(z)]\, dz, \qquad (16)$$

$$\int_0^X H_L(x)\, dx = \rho L_v \int_0^{\delta_q(X)} U(X,z)$$

$$\times [Q(X,z) - Q_i]\, dx . \qquad (17)$$

Notice that the integrations now go only to δ_h, the thermal IBL height, and to δ_q, the moisture IBL height, since by definition $T - T_i$ is zero above δ_h and $Q - Q_i$ is zero above δ_q.

Equations 16 and 17 give the total sensible and latent heat exchanged between the grass surface and the air for the area between $x = 0$ and $x = X$. I obtain estimates of the average surface fluxes ($mW\ cm^{-2}$) by dividing the two equations by the fetch:

$$H_{s2} = H_{s1} + \rho c_p X^{-1} \int_0^{\delta_h} U(T - T_i)\, dz , \qquad (18)$$

$$H_{L2} = \rho L_v X^{-1} \int_0^{\delta_q} U(Q - Q_i)\, dz , \qquad (19)$$

where $H_{s1} = \rho c_p \overline{w\theta}_i$.

After finding the downwind velocity profile using the method described in the preceding subsection, calculating the total and average downwind heat fluxes from eq 16–19 is straightforward. I connect the profile data with semilogarithmic arcs and do the indicated integration piecewise. The only troublesome point is assigning a surface roughness for the lower limit of the integrations. I use the value $z_{02} = 0.14$ cm given by RPB, setting $U(z_{02}) = 0$, $T(z_{02}) = T_{02}$, and $Q(z_{02}) = Q_{02}$. The uncertainties in T_{02} and Q_{02} that I have already discussed are not important in these integral calculations. Because RPB measured temperature and humidity within 5 cm of the surface, errors in the estimated values of T_{02} or Q_{02} could lead to errors of no more than 5% in the computed fluxes.

RESULTS

Energy budget

Table 1 lists the results of my heat flux calculations. For Runs 19 to 43 RPB included upwind and downwind measurements of both R_n and G. Figure 2

Table 1. Summary of the results of the heat flux calculations. "Up" refers to upwind of the surface change, "down" to downwind of it. L is the upwind Obukhov length, q_* the downwind friction humidity (defined in eq 38).

	Fetch	h	L	u_* (cm/s)		T_0(°C)		q_*	Flux up (mW cm^{-2})			Flux down (mW cm^{-2})			
Run	(m)	(cm)	(m)	up	down	up	down	(g/kg)	R_n	G	H_s	R_n	G	H_s	H_L
1	16.0	-	-4.61	22.2	28.7	42.2	21.6	-3.06	56.1	16.7	20.4	67.0	-	-14.1	92.8
2	18.5	-	-3.86	21.9	28.5	43.9	21.5	-3.26	46.9	-	23.4	59.0	-	-11.7	98.2
3	16.0	-	-2.68	19.0	24.3	44.2	21.9	-3.07	46.9	-	21.8	59.0	-	-14.1	78.6
4	17.4	320	-3.92	21.0	27.7	43.4	30.0	-3.40	46.0	-	20.4	52.7	-	-28.5	99.0
5	18.1	-	-2.66	17.1	22.3	42.4	22.0	-2.77	41.9	-	16.2	52.7	-	-20.9	65.0
6	18.5	238	-2.39	15.6	19.3	40.1	19.4	-2.14	30.6	-	13.5	41.4	-	-8.2	43.6
7	19.5	221	-3.41	16.7	21.6	38.8	23.6	-1.73	26.4	-	11.7	33.9	-	-19.9	39.6
8	16.5	166	-3.17	17.6	21.9	41.1	25.3	-1.85	25.5	-	14.9	33.5	-	-13.4	42.8
9	23.5	273	-2.01	13.8	17.7	38.5	23.1	-1.77	25.5	-	11.3	33.1	-	-4.7	33.4
10	21.9	218	-3.58	16.4	20.6	37.6	23.6	-1.50	26.4	-	10.6	33.1	-	-4.8	32.9
11	16.6	233	-4.67	17.5	22.0	34.5	22.3	-1.44	2.9	-	9.9	8.4	-	-22.3	34.1
12	16.8	166	-3.36	15.6	20.0	34.9	21.3	-1.29	8.8	-	9.8	15.1	-	-15.0	27.7
13	16.0	189	-3.86	18.8	23.6	38.4	26.7	-2.18	46.9	-	14.7	50.2	-	-16.0	54.8
14	16.2	172	-2.84	17.9	22.2	40.8	24.5	-2.27	53.2	-	17.4	61.5	-	-10.1	53.5
15	16.2	209	-4.94	23.2	29.1	41.9	28.4	-2.09	50.2	-	21.6	56.9	-	-12.0	64.4
16	16.2	220	-8.89	28.2	36.3	40.9	23.7	-1.97	44.8	-	21.8	53.6	-	-27.2	75.5
17	16.4	191	-6.96	25.0	32.3	41.6	23.1	-1.51	41.9	-	19.4	51.5	-	-25.6	51.4
18	18.0	252	-5.94	20.8	26.4	38.3	13.8	-1.52	16.7	-	13.0	29.3	-	-20.0	42.6
19	19.8	-	-1.05	12.9	15.5	40.7	22.2	-2.40	33.5	10.9	17.6	43.1	5.0	1.0	39.9
20	16.7	-	-3.61	19.1	24.7	38.9	21.5	-2.84	35.6	0.0	16.4	44.4	-2.1	-14.9	74.5
21	17.9	-	-1.92	14.9	18.8	39.6	26.8	-2.27	27.6	-2.1	14.7	31.4	-2.1	-5.8	45.4
22	17.8	-	-2.43	17.7	22.5	41.3	27.0	-2.52	49.8	26.8	19.4	56.9	10.0	1.7	60.1
23	17.9	-	-2.19	17.4	21.9	42.2	23.8	-2.96	56.1	23.0	20.5	65.7	10.9	-3.1	69.0
24	17.7	-	-3.09	19.4	24.9	42.1	23.1	-3.46	57.8	23.0	20.2	67.8	13.0	-21.4	91.2
25	17.7	-	-2.71	19.2	24.7	43.1	26.2	-2.89	56.1	23.0	22.2	64.9	12.1	-0.1	75.4
26	19.1	-	-3.80	20.4	27.1	40.6	19.7	-2.09	44.8	13.8	19.3	55.7	9.2	-15.1	60.1
27	16.2	212	-5.30	25.7	34.2	44.2	23.3	-2.01	41.9	10.0	27.3	53.2	7.1	-19.4	72.2
28	17.8	-	-2.76	18.0	22.9	41.7	21.1	-2.38	35.6	10.0	18.1	46.5	7.1	-6.0	57.6
29	18.1	236	-15.17	30.8	42.2	41.1	26.0	-2.27	64.0	16.7	16.4	71.6	6.7	-33.7	99.5
30	19.5	207	-15.46	32.6	42.6	41.7	27.3	-1.60	64.0	15.9	19.2	71.2	5.0	-19.5	71.3
31	16.7	190	-14.22	32.8	44.0	42.8	27.4	-2.23	62.0	15.9	21.2	69.9	5.0	-37.9	102.1
32	17.8	210	-13.78	31.5	41.8	42.3	28.8	-2.28	61.1	16.7	19.4	67.8	4.6	-37.9	99.4
33	17.4	205	-11.29	28.3	37.5	42.4	26.9	-2.33	59.9	13.4	17.2	67.8	4.6	-42.9	90.9
34	17.4	257	-8.44	26.4	35.3	43.6	25.4	-2.75	51.9	10.9	18.6	61.5	4.2	-36.5	100.8
35	18.3	191	-7.73	24.6	32.0	42.6	22.7	-2.18	48.1	9.6	16.4	58.6	4.2	-22.9	72.6
36	17.7	236	-7.78	25.9	33.8	43.7	24.9	-2.72	46.9	8.8	19.1	56.9	4.2	-38.8	95.2
37	22.2	220	-7.78	23.7	31.1	42.0	20.7	-1.77	38.1	7.1	14.6	49.4	4.2	-18.0	57.2
38	21.5	194	-7.06	21.7	28.1	41.4	19.2	-1.61	33.9	7.1	12.4	45.6	2.9	-18.0	47.0
39	20.0	287	-5.23	23.0	28.8	40.5	21.1	-2.34	44.8	7.1	19.8	54.8	0.0	-3.3	71.3
40	16.3	250	-7.43	25.8	33.7	39.5	22.1	-2.19	41.0	7.1	19.7	49.8	0.8	-15.6	78.2
41	17.7	228	-2.60	17.0	21.3	40.6	21.1	-2.66	38.5	7.1	16.2	48.6	0.0	-5.0	59.9
42	16.3	245	-4.72	22.4	28.7	41.1	21.1	-2.40	35.6	5.0	20.2	46.0	-0.8	-18.9	72.6
43	17.3	224	-4.21	18.9	24.4	38.6	19.0	-2.33	33.5	5.9	13.7	43.5	0.0	-10.5	60.2

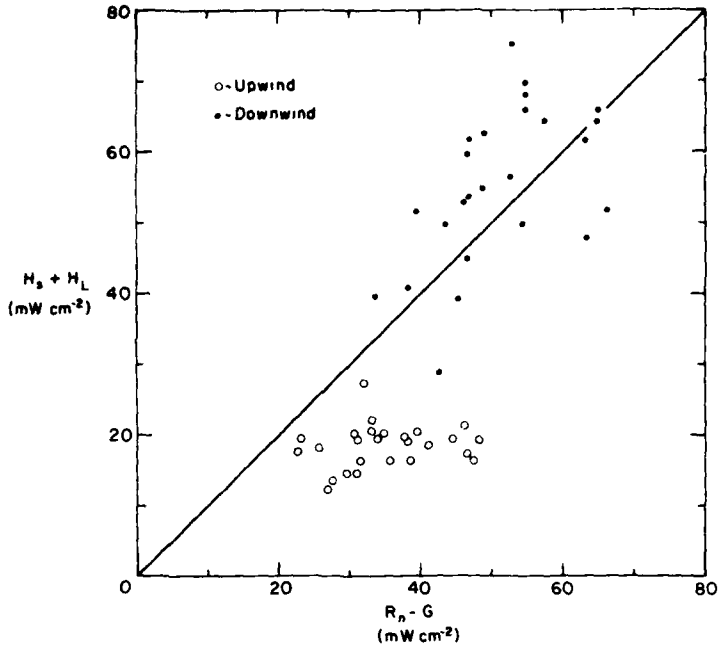

Figure 2. Comparison of the computed fluxes with the measured values of net radiation and ground heat flux.

compares these values with the fluxes I compute. The upwind surface energy budget was clearly not balanced; the downwind balance was better although $H_s + H_L$ seems somewhat large. Taylor (1971) also found the heat flux too small to balance the upwind budget for Runs 7 and 27, the only ones he considered.

Implicit in the budget equation (eq 3) is the steady-state assumption. The radiative surface temperatures RPB listed and the upwind surface temperatures I calculate suggest this may not be a good assumption. Figure 3 indicates that on 26 and 31 January 1961 the surface temperature rose to an afternoon maximum at about 1400h and then decreased. In other words, the surface was storing heat then releasing it. Approximating the storage term, we can rewrite eq 3 as

$$R_n - G - H_s - H_L - d\,\rho_e c_e \frac{\partial T}{\partial t} = 0, \qquad (20)$$

where ρ_e is the density of the tarmac, c_e is its specific heat, and d is the thickness of tarmac that undergoes heating. Equation 20 shows that the turbulent fluxes will be less than $R_n - G$ when the surface is heating up. As the surface cools, this heat loss will enhance the turbulent fluxes and they should exceed $R_n - G$. The upper traces in Figure 3 show this energy conversion qualitatively. $R_n - G - H_s$ (H_L was zero upwind) has no zero crossing, although it should if excluding the storage term were the sole reason for the imbalance. In addition, on estimating the size of the storage term by estimating $\partial T/\partial t$ from Figure 3 and using d = 1.5 cm as the thickness of the tarmac above the heat flux plate*, I find that its range, ~2 mW cm^{-2}, is too small to explain the 15 mW cm^{-2} swings in $R_n - G - H_s$. There is still an unexplained error in the upwind heat budget.

The assumption that H_L was zero upwind cannot account for this error. If the humidity profiles truly increased slightly with height, as the data show, they would require a downward flux of latent heat—a flux that would increase the energy deficit rather than decrease it. I feel that the error is not in the upwind sensible heat fluxes either. If these were large enough to balance the upwind budget, $H_s + H_L$ would be substantially larger than $R_n - G$ downwind (see eq 18). Steady state and the consequent balanced energy budget seems to be a good assumption downwind, however. The RPB radiative temperatures do

*Personal communication with E.F. Bradley, CSIRO, Canberra, Australia, 1980.

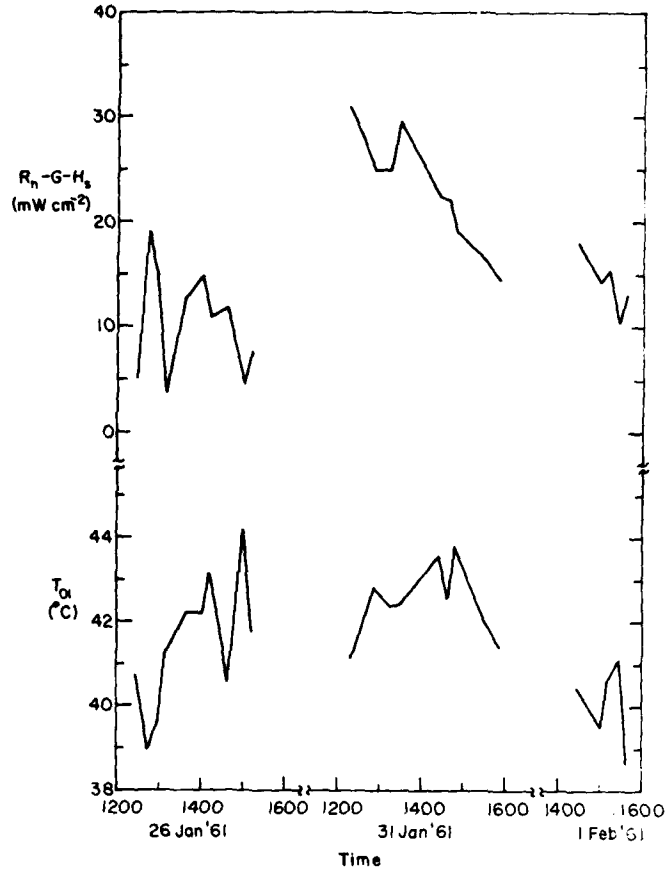

Figure 3. Temporal behavior of the calculated upwind surface temperature and of the upwind energy budget.

suggest a surface heating and cooling cycle downwind, especially on 31 January, but no interrelationship between $R_n - G - H_s - H_L$ and surface temperature exists downwind as it does upwind. Although the downwind surface temperature may have changed, evidently enough water was available to carry the excess heat away without significant storage.

I finally must consider whether the measurements of R_n and G could have been in error. Schwerdtfeger (1976) discussed the difficulties in measuring ground heat flux, but the G values tabulated by RPB appear to be the proper size when compared with similar measurements summarized by Munn (1966) and Geiger (1971). Even if the G values were systematically underestimated by 100%, however, they would still contribute too little to the budget to account for the imbalance.

Because R_n, on the other hand, is the largest term in the upwind energy budget, a systematic error in its measurement could well explain the imbalance. Using a relation given by Seckel and Beaudry (1973) to approximate total sun and sky radiation, assuming no cloud cover, and estimating incoming longwave radiation with Swinbank's (1963) formula and outgoing longwave radiation by $\epsilon_1 \sigma T_{01}^4$, I can estimate an upper bound on R_n over the tarmac. This value, 50 mW cm^{-2}, is well below some of the higher values RPB listed and thus seems to imply that their measurements may have overestimated the upwind value of R_n. Although correcting for such an error would bring the upwind energy budget into better balance, I do not feel that correction is justified: estimates of incoming longwave radiation over short time intervals from formulas originally intended for long-term averaging are too uncertain (Arnfeld 1979). I therefore leave the upwind energy budget as it is, unbalanced, and suggest that this imbalance may have resulted from errors in the

upwind measurements of R_n. All other terms in the budget are of the proper size.

Latent heat flux

Andreas et al. (1979, 1981) measured sensible heat and condensate fluxes downwind of a step change in surface heat and moisture flux. When these fluxes are nondimensionalized as Nusselt numbers (Schlichting 1968), the Nusselt numbers for both sensible heat and condensate are equal for a given flow regime. Because similar molecular processes control the transfer of both heat and moisture across an interface and in the light of results reported by Coantic and Favre (1974), Andreas et al. (1979) concluded that the latent heat flux should also obey the Nusselt number equality. Figure 4 supports their hypothesis. In it I have plotted the sensible heat flux data of Andreas et al. (1979), the condensate data of Andreas et al. (1981), and the downwind latent heat flux values calculated from the RPB data. Although Andreas et al. (1979, 1981) collected their data over arctic leads during winter, an environment in almost total contrast to that of the RPB measurements, one line fits all three data sets; though grossly dissimilar, the different regimes obeyed the same basic physics. The line in Figure 4 is

$$N = 0.08\, R_x^{0.76}, \tag{21}$$

where the fetch Reynolds number,

$$R_x = U_{200}X/\nu, \tag{22}$$

characterizes the flow. The Nusselt numbers for sensible heat N_s, latent heat N_L, and condensate N_c are defined as

$$N_s = H_s X/\kappa(T_{02} - T_{200})$$

$$= H_s X/\rho c_p D(T_{02} - T_{200}), \tag{23}$$

$$N_L = H_L X/\rho L_v D_w (Q_{02} - Q_{200}), \tag{24}$$

$$N_c = H_c X/\rho D_w (C_{02} - C_{200}). \tag{25}$$

In eq 22-25 U_{200}, T_{200}, and C_{200} are the wind speed, temperature, specific humidity, and condensate concentration (in g/g) 200 cm above the upwind surface; C_{02} is the surface condensate concentration (Andreas et al. 1981); ν, κ, D, and D_w are the kinematic viscosity, thermal conductivity, thermal diffusivity, and water vapor diffusivity in air; and H_c ; is the surface condensate flux.

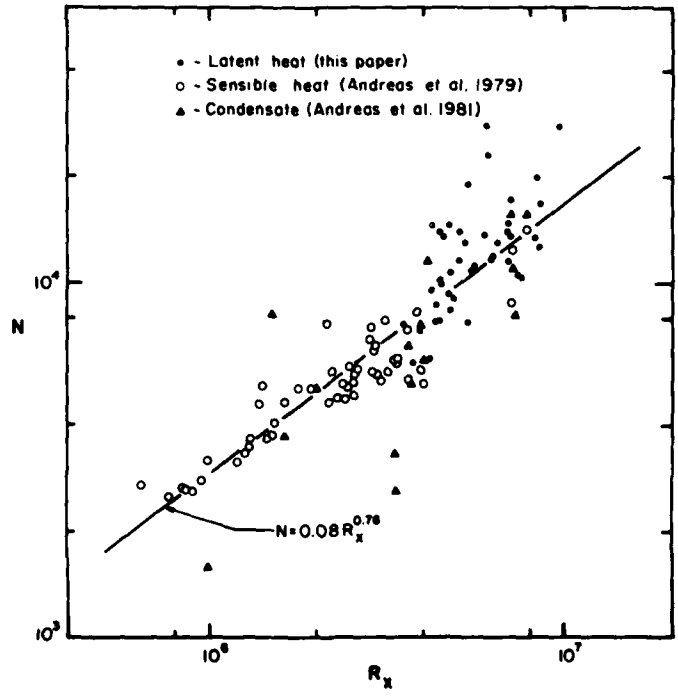

Figure 4. Nusselt numbers from three different data sets correlated with fetch Reynolds number.

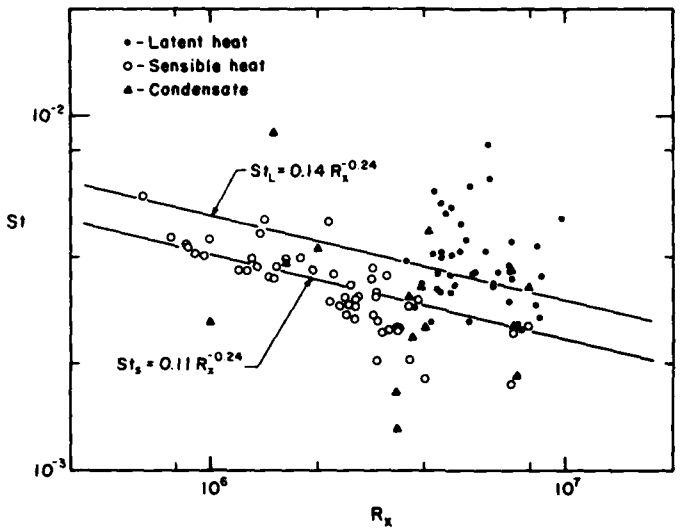

Figure 5. Stanton numbers plotted versus fetch Reynolds number. The lines are eqs 26 and 27 with eq 21 substituted for N.

Equation 21 is slightly different than eq 1, the relation Andreas et al. (1979) found using only the sensible heat flux data shown in Figure 4. Numerically, eqs 1 and 21 are very close, however; the two are nearly coincident in the fetch Reynolds number region covered by the sensible heat flux data. Because the RPB latent heat flux data neatly extend this fetch Reynolds number range, eq 21 is the more representative expression through the entire region.

One might suppose that the downwind RPB sensible heat flux should also obey eq 21. It does not. In the RPB study the sensible heat flux behaved differently than did the fluxes in the three data sets plotted in Figure 4. Each of the fluxes represented in Figure 4 went from a near-zero value upwind to a large positive value downwind. But during the RPB experiment the sensible heat flux reversed direction within the IBL: it was large and positive upwind and large and negative downwind. The slope of the temperature profile necessarily also reversed sign within the IBL. Under these circumstances, $T_{02} - T_{200}$ would not be the proper temperature scale in eq 23. There is evidently no reason, however, why eq 21 cannot describe a negative downwind flux if the upwind flux is near zero.

Stanton numbers (Schlichting 1968, p. 662), essentially bulk aerodynamic coefficients, are sometimes used instead of Nusselt numbers to parameterize fluxes in a fetch-limited flow (e.g. Mangarella et al. 1972, 1973). Stanton numbers for sensible (St_s) and latent (St_L, often called the Dalton number) heat fluxes are defined as

$$St_s = N_s R_x^{-1} P^{-1} \tag{26}$$

and

$$St_L = N_L R_x^{-1} Sc^{-1}, \tag{27}$$

where P is the Prandtl number, and Sc is the Schmidt number. For a particular flow regime—a particular fetch Reynolds number—$N_s = N_L$; hence,

$$St_L = (P/Sc)St_s = (D_w/D)St_s . \tag{28}$$

Because $D_w > D$ (List 1963), the Stanton numbers will not be equal. Figure 5 confirms this Stanton number inequality and so emphasizes the advantages of using the Nusselt number as a flux parameter. The lines in the figure are eq 26 and 27 with eq 21 substituted for N. The results reported by Mangarella et al. (1972, 1973) also indicate this Stanton number inequality. Although in their results St_L is seldom 20% larger than St_s as required by the value of D_w/D, it is systematically larger.

Surface stress

I have explained how I found the upwind friction velocity u_{*up}. After determining downwind velocity profiles, I computed the downwind friction velocity

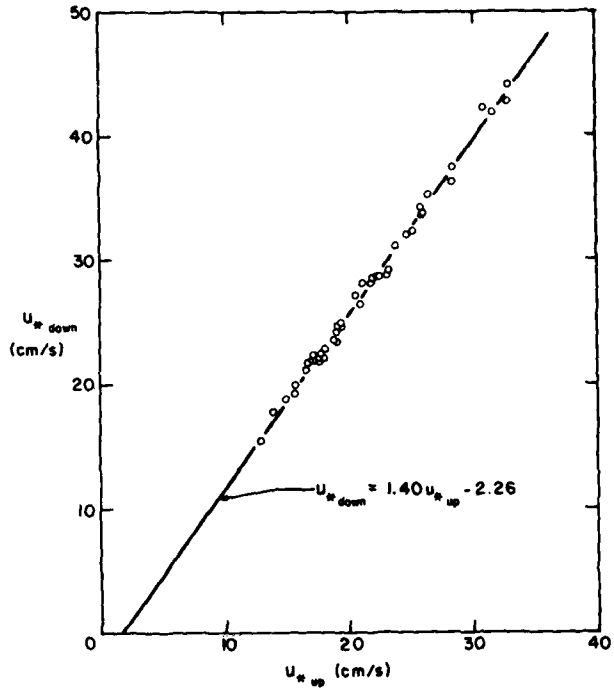

Figure 6. Correlation between the calculated values of upwind and downwind friction velocity.

u_{*down} by fitting a least-squares line through the lowest three profile levels, $U(z_{02}) = 0$, $U(27.5)$, and $U(37.5)$. Bradley (1972) demonstrated that for profile levels near the surface, as these are, the computed value of u_* will be within 1% of the actual value regardless of stability.

Figure 6 compares downwind and upwind values of u_*. The result,

$$u_{*down} = 1.40\,u_{*up} - 2.26, \qquad (29)$$

which gives u_{*down} in cm/s for u_{*up} in cm/s, is not consistent with the RPB result $u_{*down}/u_{*up} \sim 1.7$. Equation 29 is in good agreement with the results of Taylor (1971) for Run 7, $u_{*down}/u_{*up} \sim 1.43$, and of Rao et al. (1974) for Run 6, $u_{*down}/u_{*up} \sim 1.40$, however. The magnitude of the discrepancy between the RPB result and mine (i.e. 1.7/1.4) is entirely compatible with the difference in z_0 values ascribed to the tarmac. Previously I explained why the z_0 value RPB found for the tarmac, 0.002 cm, seemed too small. The smallness of this value goes hand in hand with an underestimate of u_{*up} and so with an overestimates of u_{*down}/u_{*up}.

The implications of Bradley's (1972) research are that we can define a meaningful drag law regardless of stability and even in a developing flow if we choose a reference height low enough. Figure 7 shows that drag law for the downwind RPB data,

$$u_{*down} = 0.0646\,U_{50} + 0.37\,. \qquad (30)$$

Here u_{*down} is in cm/s when U_{50}, the wind speed 50 cm above the surface at fetch X, is in cm/s. This result is in excellent agreement with ones reported by Andreas et al. (1979) for flow over arctic leads,

$$u_{*down} = 0.0643\,U_{50} - 0.77, \qquad (31)$$

and by Hicks (1976) for more homogeneous Australian grassland,

$$u_* = 0.0632\,U_{50} + 2.22\,. \qquad (32)$$

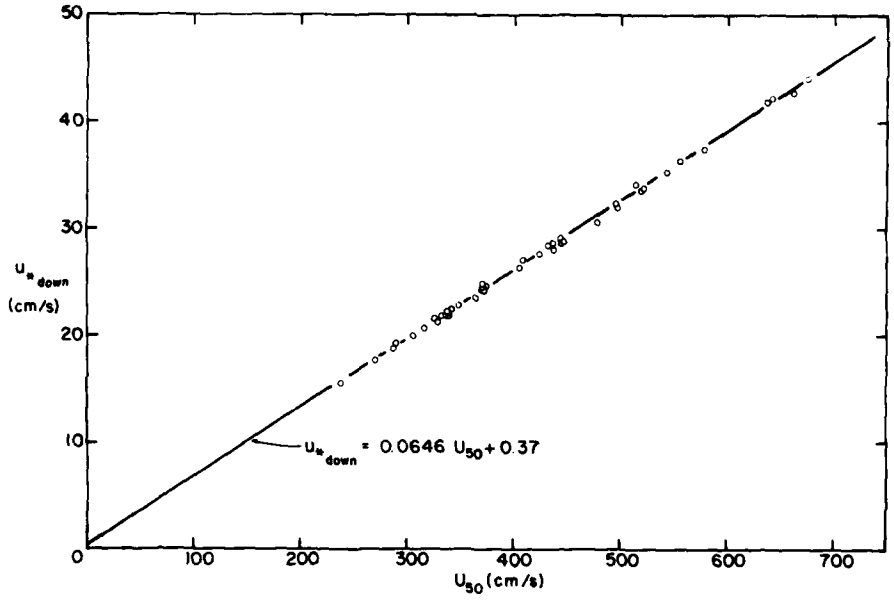

Figure 7. Downwind drag relation.

Downwind humidity profiles

One of my principal reasons for undertaking the analysis of the RPB data was an interest in the humidity profile following a step change in surface moisture. We had argued earlier (Andreas et al. 1981) that the condensate scale $\hat{c}$ in the nondimensional condensate gradient over arctic leads,

$$\phi_c = (z/\hat{c})\,\frac{\partial C(z)}{\partial z}\ , \qquad (33)$$

is a function of two length scales, height and fetch. When we modeled $\hat{c}$ as

$$\hat{c}(X,z) \propto \ln[z/h(x)]\,,\ z_0 \ll z \ll h\,, \qquad (34)$$

where h is a fetch-dependent estimator of IBL height, we found that the condensate profile should have the form

$$C(z)^{1/2} \propto \ln(z/h)\,. \qquad (35)$$

The measured profiles substantiated these heuristic arguments and also yielded the proportionality constant in eq 35. We found

$$[-C(z)/c_*]^{1/2} = -0.34\,\ln(z/h), \qquad (36)$$

with c_* defined from the surface value of the condensate flux. The excellent set of humidity profiles collected by RPB gave me a chance to test this model on another scalar quantity.

Figure 8 shows that 30 of the 43 RPB humidity profile sets follow an equation like eq 36. The line in the figure is

$$[-\Delta Q/q_*]^{1/2} = -0.37\,\ln(z/h),$$

$$z_0 \ll z \ll h\,, \qquad (37)$$

where $\Delta Q = Q(X,z) - Q_i(z)$ and

$$q_* = -H_{L2}/\rho L_v k\, u_{*down}\,, \qquad (38)$$

H_{L2} being the downwind latent heat flux calculated with eq 19.

The multiplicative constants in eqs 36 and 37 are slightly different. I suspect that the source of this difference is the difference in z_0 values. The multiplicative constant is evidently only a weak function of z_0/h, however; with the small spread in the z_0/h ratios of the lead and RPB data sets, I can say little about its behavior except that a conservative range for it in naturally occurring internal boundary layers is [0.28, 0.42].

The estimate of IBL height h was found by plotting each humidity profile as $\Delta Q^{1/2}$ vs ln z and extending the best straight line through this profile to $\Delta Q^{1/2} = 0$. Figure 9, which contains data for both condensate

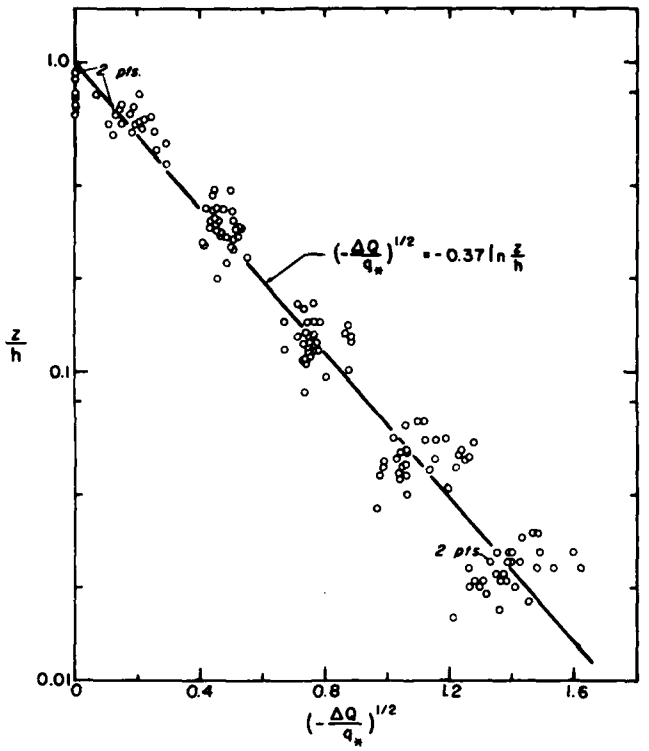

Figure 8. Nondimensional humidity-difference profiles. The 30 profiles quality-coded 1 or 2 are shown here.

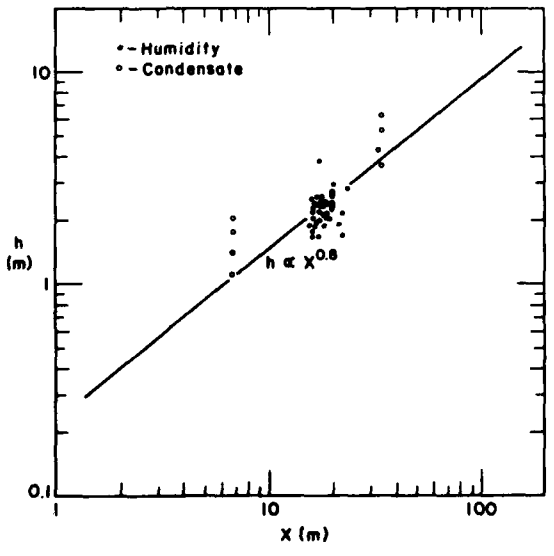

Figure 9. IBL height vs fetch for both the condensate data of Andreas et al. (1981) and the 30 humidity profiles shown in Figure 8.

profiles (Andreas et al. 1981) and the RPB humidity profiles, shows that, as expected, h is a function of X. The line is drawn by eye so that h is proportional to $X^{0.8}$ (Sutton 1934, 1953, Calder 1949, Elliot 1958, Philip 1959). It is customary to nondimensionalize plots of IBL height vs fetch with a surface roughness scale. The correlation in our data does not improve with any such nondimensionalization, however; the scaling lengths must, therefore, be nearly the same for both data sets. Indeed, the scalar roughness lengths, z_w, computed by the method suggested by Garratt and Hicks (1973, Fig. 1) are 0.025 cm and 0.023 cm for condensate and humidity, respectively. Choosing $z_w = 0.025$, the line in Figure 9 becomes

$$h/z_w = 1.21\ (X/z_w)^{0.8}\ . \qquad (39)$$

The research by Andreas et al. (1981) and this study, are, to my knowledge, the only geophysical-scale experimental studies of IBL growth for passive, scalar contaminants. Therefore, although the x-dependence of the IBL height shown in eq 39 is on

Table 2. Quality codes of the ΔQ profiles, and wind direction during each run. The meaning of the quality codes is given in the text.

Run	Date	Quality	Direction (°)
1	10 Jan 61	3	0
2		3	-30
3		3	0
4		1	-23
5		3	-28
6	11 Jan 61	2	-30
7		1	-35
8		1	-14
9		1	-47
10		1	-43
11	13 Jan 61	2	-15
12		1	-18
13		2	0
14		1	-8
15		1	-8
16		1	-10
17		2	-12
18		2	-27
19	26 Jan 61	3	36
20		3	17
21		3	27
22		3	26
23		3	27
24		3	25
25		3	25
26		3	33
27		1	10
28		3	26
29	31 Jan 61	1	-28
30		2	-35
31		2	-17
32		1	-26
33		1	-23
34		1	-23
35		1	-29
36		1	-25
37		1	-44
38		1	-42
39	11 Feb 61	1	-37
40		1	12
41		1	-25
42		1	-12
43		1	22

sound footing, the multiplicative constant must remain tentative. Elliott's (1958) model for temperature as a passive contaminant and calculations by Dyer (1963)—based on Philip's (1959) theory of local advection—indicated a constant much smaller than that shown in eq 39. In other words, these theories predicted that the IBL grows more slowly with fetch than the experimental evidence shows. Data reported by Peterson et al. (1976), however, seem to support my findings; the internal momentum boundary layer they studied grew higher than expected on the basis of numerical models. Further experimental work, with emphasis on a consistent definition of IBL height and a uniform choice of scaling length, is necessary to clarify these conflicting results.

Thirty of the 43 RPB humidity-difference profiles were proportional to $(\ln z)^2$. I have quality coded each profile with a number from one to three: 1) the profile is well represented by $\Delta Q^{1/2} \propto \ln z$, 2) four of the five profile points show $\Delta Q^{1/2} \propto \ln z$, and 3) $\Delta Q^{1/2} \propto \ln z$ is not indicated. Figure 8 contains the 30 profiles that were assigned quality codes of 1 or 2. On sorting the runs out as in Table 2, we get some insight into why all the profiles did not follow eq 37. The 13 contrary profiles were collected on only two of the six experimental days, 10 January and 26 January. And these profiles account for 13 of the 15 profiles collected on those days. This systematic behavior suggests that an experimental or calibration error on each of these two days could have masked the $(\ln z)^2$ behavior of the humidity-difference profiles. If only two of the 20 thermocouples RPB used to measure upwind and downwind wet and dry bulb temperatures had bias errors, the $\Delta Q^{1/2} \propto \ln z$ profile form would have been lost. The evidence that such errors occurred on, at most, two days is testimony to the experimental care Rider, Philip, and Bradley took.

Table 2 also suggests that the quality of the humidity profiles may have been influenced by wind direction. On 26 January—when nine of the ten profiles were quality 3—the wind direction was positive (0° is along the site axis). During only two of the remaining 33 runs was the wind direction positive. This is strong circumstantial evidence that the flow was not in equilibrium with the tarmac when its direction was ~ 30° but was apparently disturbed by the large buildings upwind in that direction. RPB explained, in fact, that even when the wind direction was nearer 0°, these buildings were the source of "odd gusts." I feel, therefore, that flow distortion by these buildings voided the upwind-equilibrium assumption on 26 January, resulting in the poor quality of the humidity profiles on that day.

DISCUSSION

Results in the last section present a paradox. The Nusselt numbers for three different scalar fluxes,

sensible heat, latent heat, and condensate, obey the same fetch Reynolds number relation, but temperature profiles over arctic leads do not have the same form as the condensate and RPB humidity profiles. One set of results suggests that scalar quantities are transferred similarily in an IBL, while a second set of results shows inherent differences in the transfer. On the basis of current boundary layer theory, these results are not really incompatible, however. The scalar quantities we have studied are transferred across a surface by virtually identical molecular processes—which transfer determines the Nusselt number. But they need not obey similar physics in the turbulent IBL, where the profiles were measured.

Although I have computed the downwind surface fluxes from the measured profiles according to eq 18 and 19, eq 16, 17 and 23-25 show that the surface flux of a scalar S is related to the Nusselt number by

$$N_S = D_S^{-1}(S_0 - S_{200})^{-1}\int_0^X H_S(x,z=0)\,dx\,. \tag{40}$$

Here D_S is the molecular diffusivity of the scalar; S_0, its surface value; S_{200}, its value 200 cm above the upwind surface; and H_S is now the kinematic surface flux (i.e. with constants such as ρc_p and ρL_v omitted).

H_S can be computed from the S gradient through the molecular sublayer,

$$H_S(x,z=0) = -D_S\left.\frac{\partial S\,(x,z)}{\partial z}\right|_{z=0}. \tag{41}$$

Schlichting (1968, p. 284) showed that a scaling length for z in fetch-limited boundary layers is $(\nu x/U_{200})^{1/2}$. Such a scaling length seems appropriate in Nusselt number computations for any of the scalars we are discussing, because for large R_x the Nusselt number cannot depend on stability (Andreas 1980). With this z-scale in eq 41, eq 40 becomes

$$N_S = R_x^{1/2}\int_0^1 \tilde{x}^{-1/2}\left.\frac{\partial\tilde{S}\,(\tilde{x},\tilde{z},R_x,\nu/D_S)}{d\tilde{z}}\right|_{\tilde{z}=0} d\tilde{x}\,, \tag{42}$$

where the wavy overbars indicate new nondimensional quantities: $\tilde{x} = x/X$, $\tilde{z} = (z^2U_{200}/\nu x)^{1/2}$, and $\tilde{S} = (S - S_{200})/(S_0 - S_{200})$.

Schlichting (1968) went on to show that in an IBL the nondimensional temperature profile evaluated at the surface, $\partial\tilde{T}/\partial\tilde{z}\,|_{z=0}$, is a weak function of Prandtl number ($\sim P^{1/3}$). If the nondimensional profiles of the other scalars are also only weak functions of their molecular diffusivities—as is temperature—and if the scaling performed in the preceding paragraph is appropriate for all the scalars, eq 42 implies that the corresponding Nusselt numbers will be nearly identical functions of the fetch Reynolds number in the IBL. The Nusselt number equality that we have found is a posteriori evidence for the validity of these assumptions; there is similarity in the transport of scalars through a surface molecular sublayer. The predicted dependence of N on molecular diffusivity is such a small effect that it is lost amid the experimental uncertainties.

In the turbulent IBL, on the other hand, the transfer processes need not be the same for each scalar. Warhaft (1976) has developed a simple model for turbulent transfer in a horizontally homogeneous surface layer. Although his model is not directly applicable to internal boundary layers, it does indicate the likelihood of differences in the turbulent transfer of scalars: differences that are here our concern. We can thus gain some insight from his model. The equations that Warhaft (1976) derived for the turbulent fluxes of temperature and humidity are

$$\overline{w\theta} = -K\left[\frac{\partial T}{\partial z} - \tfrac{1}{2}(g/\overline{w^2})(\overline{\theta^2}/T_0 + 0.61\,\overline{\theta q})\right] \tag{43a}$$

and

$$\overline{wq} = -K\left[\frac{\partial Q}{\partial z} - \tfrac{1}{2}(g/\overline{w^2})(0.61\,\overline{q^2} + \overline{\theta q}/T_0)\right]. \tag{43b}$$

Here T_0 is a temperature representative of the surface layer; and $K = \tfrac{1}{2}(\overline{w^2}\,\overline{e}/\epsilon\Lambda)$, where $\overline{e}$ $(=\overline{u^2} + \overline{v^2} + \overline{w^2})$ is the turbulent kinetic energy, ϵ is the energy dissipation rate, and Λ is a dimensionless constant.

I nondimensionalize eq 43 with the standard deviations of temperature, $\sigma_\theta = \overline{\theta^2}^{1/2}$, humidity, $\sigma_q = \overline{q^2}^{1/2}$, and vertical velocity, $\sigma_w = \overline{w^2}^{1/2}$, and with the temperature-humidity correlation coefficient, $\rho_{\theta q} = \overline{\theta q}/\sigma_\theta\,\sigma_q$:

$$\overline{w\theta}/\sigma_w\sigma_\theta = -(gK/\sigma_w^3)[(\sigma_w^2/g\sigma_\theta)\frac{\partial T}{\partial z} - \tfrac{1}{2}(\sigma_\theta/T_0 + 0.61\,\sigma_q\,\rho_{\theta q})]\,, \tag{44a}$$

$$\overline{wq}/\sigma_w\sigma_q = -(gK/\sigma_w^3)[(\sigma_w^2/g\sigma_q)\frac{\partial Q}{\partial z} - \tfrac{1}{2}(\sigma_\theta\,\rho_{\theta q}/T_0 + 0.61\,\sigma_q)]\,. \tag{44b}$$

If $\rho_{\theta q} = 1$, these two equations have identical nondimensional forms. The fluxes then clearly result from two sources, a flux down the scalar gradient and a nongradient component associated with the turbulence. Notice that, depending on its sign, the scalar gradient can drive an upward or a downward flux; but the nongradient flux is always upward—hence, at times it is countergradient (Deardorff 1972).

On rearrangement, eq 44a and 44b yield the nondimensional gradients:

$$-(\sigma_w^2/g\alpha_\theta)\frac{\partial T}{\partial z} = \sigma_w^2\,\overline{w\theta}/gK\sigma_\theta - \tfrac{1}{2}(\sigma_\theta/T_0 + 0.61\,\sigma_q\,\rho_{\theta q}) ,$$

(1a) (2a) (3a) (45a)

$$-(\sigma_w^2/g\sigma_q)\frac{\partial Q}{\partial z} = \sigma_w^2\,\overline{wq}/gK\sigma_q - \tfrac{1}{2}(\sigma_\theta\,\rho_{\theta q}/T_0 + 0.61\,\sigma_q) .$$

(1b) (2b) (3b) (45b)

From these it is evident that the scalar profiles are determined by both the boundary conditions (terms 2a and 2b) and the turbulence within the layer (terms 3a and 3b). The nondimensional profiles will, therefore, be dissimilar if any one of the following is true:

1. If the boundary conditions are different—for example, if $\overline{wq}$ is positive and $\overline{w\theta}$ is negative.
2. If the temperature and humidity fluctuations are large but poorly correlated.
3. If the buoyancy effects induced by the turbulence are negligible in either eq 45a or 45b, i.e., if either term 3a or 3b can be ignored, but not both.

Experimental work by McBean and Miyake (1972), McBean (1973), and Friehe et al. (1975) corroborates these theoretical conclusions.

The humidity variance is rarely large enough to contribute to the buoyancy terms (3a or 3b) in eq 45a and 46b (Friehe et al. 197 humidity is usually a passive scalar with respect to the transports of both temperature and humidity. Temperature is also passive with regard to humidity if $|\rho_{\theta q}|$ is small and σ_θ is not extremely large. Only when $\sigma_\theta/2T_0$ is an appreciable fraction of term 1a does temperature act as an active scalar in the temperature equation.

These criteria for judging whether scalars are active or passive extend those usually seen in the literature. For example, McBean and Miyake (1972) wrote, "A passive scalar is a scalar whose variations do not significantly affect the buoyancy of a parcel of air. An active scalar is a scalar whose variations do affect the buoyancy." Through eq 45a and 45b I have shown, however, that a particular scalar can contribute to the buoyancy transfer of one scalar quantity yet not to another. Such a scalar is neither totally active nor totally passive.

Although we must be cautious in drawing inferences about scalar transfer in internal boundary layers from eq 45a and 45b, their buoyancy and gradient terms, at least, cannot be wrong. The equations thus provide some insight into the profile results discussed in the *Downwind humidity profiles* section. The RPB temperature and humidity profiles within the IBL will clearly be different because the boundary conditions are different; $\overline{w\theta}$ is downward at the grass surface and upward near the top of the IBL, while $\overline{wq}$ is upward everywhere. $\rho_{\theta q}$ will change from negative to positive as the height increases, and I suspect its absolute value will consequently be small. Term 3b should thus be negligible—buoyancy does not affect humidity transfer for the RPB data.

Condensate over arctic leads should obey a transfer equation just like that for humidity. Andreas et al. (1981) have shown that, because of the necessity of diffusion through a molecular boundary layer surrounding a condensate droplet, droplets over leads change little in size for several seconds despite step changes in ambient humidity or temperature. Over leads, away from the immediate vicinity of the surface, condensate is thus a quasi-conservative property and will obey the same diffusion equation as temperature and humidity (Pasquill 1974). A condensate transfer equation analogous to that for humidity (eq 45b) then follows directly. But again the buoyancy term will likely be negligible. Although the temperature variance over leads can be extreme—0.6 to 1.0°C^2—the correlation between temperature and condensate should be small, since a positive temperature fluctuation, for example, would lower the probability of formation of a condensate droplet by lowering the relative humidity. And I have already mentioned how slowly the small condensate droplets respond to changes in humidity and temperature. Consequently, as with humidity during the RPB experiment, buoyancy does not affect condensate transfer: both scalars should obey the same physics.

For temperature and humidity over leads, in contrast, the buoyancy term contributes several percent to both transfer equations because of the large value of σ_θ and the high temperature-humidity correlation over the warm, evaporating surface (e.g. Phelps and Pond 1971, Friehe et al. 1975; Wesely and Hicks 1978). Thus, though the boundary conditions on $\overline{w\theta}$, $\overline{wq}$, and $\overline{wc}$ over leads and on $\overline{wq}$ in the RPB experiment are the same, the corresponding scalar profiles will not all be similar. Temperature and humidity profiles should scale similarly, and the condensate and RPB humidity profiles should scale similarly, but the two groups must differ because the latter are unaffected by buoyancy.

CONCLUSIONS

The well-respected data set of Rider et al. (1963) is a standard with which to test models of flow following a step change in surface conditions. For each run in the data set I have calculated several quantities that have not been reported before. Principal among these are the sensible and latent heat fluxes and friction velocity upwind and downwind.

The upwind surface energy budget is not balanced in the steady-state form. Including a storage term qualitatively improves the balance, but there is still a discrepancy that may be due to an error in the upwind measurement of net radiation. The downwind energy budget is in approximate steady-state balance.

The surface latent heat flux, which goes from virtually zero upwind to a large upward value downwind, is related to the fetch Reynolds number. When the latent heat is nondimensionalized as a Nusselt number,

$$N_L = 0.08\, R_x^{0.76} . \qquad (46)$$

This expression is essentially the same as one found to describe sensible heat and condensate fluxes over arctic leads. I conclude that all Nusselt numbers nondimensionalizing scalar surface fluxes following a step increase in the flux are equal for a given flow regime.

The RPB humidity-difference profiles are well-represented by

$$[-\Delta Q/q_*]^{1/2} = -0.37 \ln(z/h) , \qquad (47)$$

where h is a fetch-dependent indicator of internal boundary layer height. This form of the humidity-difference profile, with the exception of the multiplicative constant, is identical to that found for condensate profiles at the downwind edge of arctic leads. The common links between these two scalars are that they have similar boundary conditions and neither is affected by buoyancy transfer. I recommend looking for this relationship in the profiles of other such scalars in fetch-limited flows.

Equations 46 and 47 imply two distinct methods of estimating the latent heat flux in fetch-limited flows from easily measured quantities. Equation 46 calls for the following five measurements: surface temperature (for computing Q_{02}, ρ, ν, L_v, and D_w), wind speed at 2 m, upwind humidity, fetch, and atmospheric pressure (also needed to find ρ). Seven measurements are necessary for determining the flux from eq 47: upwind humidity at two heights, downwind humidity at the same two heights, surface temperature (for computing ρ and L_v), wind speed 50 cm above the downwind surface (which gives u_* [eq 30]), and pressure (again for ρ). Although this second method requires two more measurements than the first, it yields two more quantities, u_* and the IBL height h.

Some of my results are not consistent with the data reported in RPB and so raise questions about the accuracy of their data. The most striking example of possible inaccuracies is in the humidity profiles of 10 January and 26 January. As I have explained, there was evidently either a calibration error on those days or the flow was disturbed by buildings upwind. The upwind value of z_0 (0.002 cm) RPB gave is very small. I feel it is too small; using it I could not retrieve reasonable upwind and downwind velocity profiles from the average profiles RPB listed. A value of $z_0 = 0.01$ cm upwind leads to upwind and downwind profiles that compare well with the few individual profiles available and is more compatible with aerodynamic considerations. The value of 1.7 RPB quoted for the ratio u_{*down}/u_{*up} is significantly larger than the value of 1.4 I would give it on the basis of eq 29. This disparity is a consequence primarily of the larger z_0 value I ascribe to the upwind tarmac. Lastly, I compute downwind surface temperatures lower than RPB measured. My values are consistent with the downwind temperature and humidity profiles, while the surface temperatures of RPB imply a complex shape for the temperature profile and a grass surface well below saturation.

LITERATURE CITED

Andreas, E.L. (1980) Estimation of heat and mass fluxes over arctic leads. *Monthly Weather Review*, vol. 108, p. 2057-2063.

Andreas, E.L., C.A. Paulson, R.M. Williams, R.W. Lindsay and J.A. Businger (1979) The turbulent heat flux from arctic leads. *Boundary-Layer Meteorology*, vol. 17, p. 57-91.

Andreas, E.L., R.M. Williams and C.A. Paulson (1981) Observations of condensate profiles over arctic leads with a hot-film anemometer. *Quarterly Journal of the Royal Meteorological Society*, vol. 107, p. 437-460.

Arnfeld, A.J. (1979) Evaluation of empirical expressions for the estimation of hourly and daily totals of atmospheric longwave emission under all sky conditions. *Quarterly Journal of the Royal Meteorological Society*, vol. 105, p. 1041-1052.

Bradley, E.F. (1972) The influence of thermal stability on a drag coefficient measured close to the ground. *Agricultural Meteorology*, vol. 9, p. 183-190.

Busch, N.E. (1973) On the mechanics of atmospheric turbulence. *Workshop on micrometeorology* (D.A. Haugen, Ed.), American Meteorological Society, p. 1-65.

Businger, J.A. (1973) Turbulent transfer in the atmospheric surface layer. *Workshop on micrometeorology* (D.A. Haugen, Ed), American Meteorological Society, p. 67-100.

Businger, J.A., J.C. Wyngaard, Y. Izumi and E.F. Bradley (1971) Flux-profile relationships in the atmospheric surface layer. *Journal of the Atmospheric Sciences*, vol. 28, p. 181-189.

Calder, K.L. (1949) Eddy diffusion and evaporation in flow over aerodynamically smooth and rough surfaces: A treatment based on laboratory laws of turbulent flow with special reference to conditions in the lower atmosphere. *Quarterly Journal of Mechanics and Applied Mathematics*, vol. 2, p. 153-176.

Coantic, M. and A. Favre (1974) Activities in, and preliminary results of, air-sea interactions research at I.M.S.T. In *Advances in Geophysics* (F.N. Frenkiel and R.E. Munn, Eds.), New York: Academic Press, vol. 18A, p. 391-405.

Deardorff, J.W. (1972) Theoretical expression for the countergradient heat flux. *Journal of Geophysical Research*, vol. 77, p. 5900-5904.

Dyer, A.J. (1963) The adjustment of profiles and eddy fluxes. *Quarterly Journal of the Royal Meteorological Society*, vol. 89, p. 276-280.

Elliott, W.P. (1958) The growth of the atmospheric internal boundary layer. *Transactions, American Geophysical Union*, vol. 39, p. 1048-1054.

Friehe, C.A., J.C. LaRue, F.H. Champagne, C.H. Gibson and G.F. Dreyer (1975) Effects of temperature and humidity fluctuations on the optical refractive index in the marine boundary layer. *Journal of the Optical Society of America*, vol. 65, p. 1502-1511.

Garratt, J.R. and B.B. Hicks (1973) Momentum, heat and water vapour transfer to and from natural and artificial surfaces. *Quarterly Journal of the Royal Meteorological Society*, vol. 99, p. 680-687.

Geiger, R. (1971) *The climate near the ground.* Cambridge, Massachusetts: Harvard University Press.

Hicks, B.B. (1976) Wind profile relationships from the "Wangara" experiment. *Quarterly Journal of the Royal Meteorological Society*, vol. 102, p. 535-551.

Kondratyev, K.Ya. (1969) *Radiation in the atmosphere.* New York: Academic Press.

List, R.J. (1963) *Smithsonian meteorological tables.* 6th ed., Washington, D.C.: Smithsonian Institution.

Mangarella, P.A., A.J. Chambers, R.L. Street and E.Y. Hsu (1972) Laboratory and field interfacial energy and mass flux and prediction equations. *Journal of Geophysical Research*, vol. 77, p. 5870-5875.

Mangarella, P.A., A.J. Chambers, R.L. Street and E.Y. Hsu (1973) Laboratory studies of evaporation and energy transfer through a wavy air-water interface. *Journal of Physical Oceanography*, vol. 3, p. 93-101.

McBean, G.A. (1973) Comparison of turbulent transfer processes near the surface. *Boundary-Layer Meteorology*, vol. 4, p. 265-274.

McBean, G.A. and M. Miyake (1972) Turbulent transfer mechanisms in the atmospheric surface layer. *Quarterly Journal of the Royal Meteorological Society*, vol. 98, p. 383-398.

Munn, R.E. (1966) *Descriptive micrometeorology.* New York: Academic Press.

Pasquill, F. (1974) *Atmospheric diffusion.* Chichester, England: Ellis Horwood Limited.

Paulson, C.A. (1970) The mathematical representation of wind speed and temperature profiles in the unstable atmospheric surface layer. *Journal of Applied Meteorology*, vol. 9, p. 857-861.

Peterson, E.W., L. Kristensen and C.-C. Su (1976) Some observations and analysis of wind over nonuniform terrain. *Quarterly Journal of the Royal Meteorological Society*, vol. 102, p. 857-867.

Phelps, G.T., and S. Pond (1971) Spectra of temperature and humidity fluctuations and of the fluxes of moisture and sensible heat in the marine boundary layer. *Journal of the Atmospheric Sciences*, vol. 28, p. 918-928.

Philip, J.R. (1959) The theory of local advection. *Journal of Meteorology*, vol. 16, p. 535-547.

Rao, K.S., J.C. Wyngaard and O.R. Coté (1974) Local advection of momentum, heat, and moisture in micrometeorology *Boundary-Layer Meteorology*, vol. 7, p. 331-348.

Razumovskii, I.T. and O.I. Popov (1974) Emissivity of certain materials in the 8.5-13.5 micron spectral region. *Atmospheric radiation studies* (K.Ya. Kondratyev, Ed.), Jerusalem: Keter Publishing House, p. 180-181.

Rider, N.E., J.R. Philip and E.F. Bradley (1963) The horizontal transport of heat and moisture—a micrometeorological study. *Quarterly Journal of the Royal Meteorological Society*, vol. 89, p. 507-531.

Rider, N.E., J.R. Philip and E.F. Bradley (1965) Horizontal transport of heat and moisture—a micrometeorological study [discussion]. *Quarterly Journal of the Royal Meteorological Society*, vol. 91, p. 236-240.

Schlichting, H. (1968) *Boundary-layer theory.* New York: McGraw-Hill.

Schwerdtfeger, P. (1976) *Physical principles of micrometeorological measurements.* Amsterdam: Elsevier.

Seckel, G.R. and F.H. Beaudry (1973) The radiation from sun and sky over the North Pacific Ocean [abstract]. *Transactions, American Geophysical Union*, vol. 54, p. 1114.

Siegel, R. and J.R. Howell (1972) *Thermal radiation heat transfer.* New York: McGraw-Hill.

Sutton, O.G. (1934) Wind structure and evaporation in a turbulent atmosphere. *Proceedings of the Royal Society, London*, vol. A146, p. 701-722.

Sutton, O.G. (1953) *Micrometeorology.* New York: McGraw-Hill.

Swinbank, W.C. (1963) Long-wave radiation from clear skies. *Quarterly Journal of the Royal Meteorological Society*, vol. 89, p. 339-348.

Taylor, P.A. (1971) Air flow above changes in surface heat flux, temperature and roughness; an extension to include the stable case. *Boundary-Layer Meteorology*, vol. 1, p. 474-497.

Townsend, A.A. (1965) The response of a turbulent boundary layer to abrupt changes in surface conditions. *Journal of Fluid Mechanics*, vol. 22, p. 799-822.

Warhaft, Z. (1976) Heat and moisture flux in the stratified boundary layer. *Quarterly Journal of the Royal Meteorological Society*, vol. 102, p. 703-707.

Wesely, M.L. and B.B. Hicks (1978) High-frequency temperature and humidity correlation above a warm wet surface. *Journal of Applied Meteorology*, vol. 17, p. 123-128.

Wieringa, J. (1980) A reevaluation of the Kansas mast influence on measurements of stress and cup anemometer overspeeding. *Boundary-Layer Meteorology*, vol. 18, p. 411-430.

Yaglom, A.M. (1977) Comments on wind and temperature flux-profile relationships. *Boundary-Layer Meteorology*, vol. 11, p. 89-102.

Zilitinkevich, S.S. (1966) Effect of humidity stratification on hydrostatic stability. *Izvestiya, Atmospheric and Oceanic Physics*, vol. 2, p. 655-658.

A facsimile catalog card in Library of Congress MARC format is reproduced below.

Andreas, Edgar L.
Sensible and latent heat fluxes and humidity profiles following a step change in surface moisture / by Edgar L. Andreas. Hanover, N.H.: U.S. Cold Regions Research and Engineering Laboratory; Springfield, Va.: available from National Technical Information Service, 1982.
vii, 24 p., illus.; 28 cm. (CRREL Report 82-12.)
Prepared for Office of the Chief of Engineers by Corps of Engineers, U.S. Army Cold Regions Research and Engineering Laboratory under DA Project 4A1611 02AT24.
Bibliography: p. 16.
1. Heat flux. 2. Humidity. 3. Micrometeorology. 4. Surface properties. I. United States. Army. Corps of Engineers. II. Army Cold Regions Research and Engineering Laboratory, Hanover, N.H. III. Series: CRREL Report 82-12.

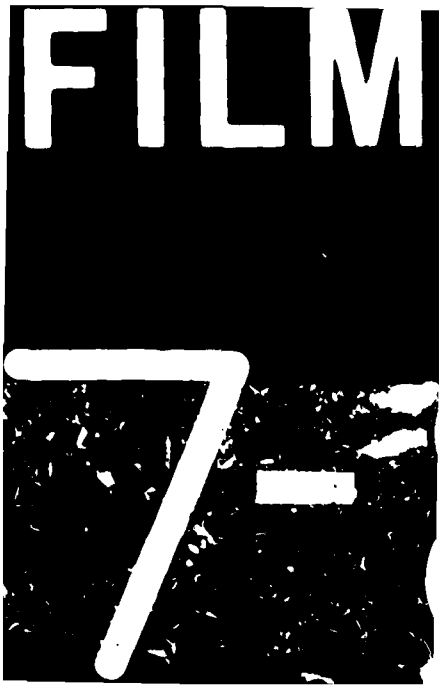
FILM
7-